1521-0103/351/2/250–258$25.00
THE JOURNAL OF PHARMACOLOGY AND EXPERIMENTAL THERAPEUTICS

http://dx.doi.org/10.1124/jpet.114.217869
J Pharmacol Exp Ther 351:250–258, November 2014

Efavirenz Induces Neuronal Autophagy and Mitochondrial Alterations

Phillip R. Purnell and Howard S. Fox

Department of Pharmacology and Experimental Neuroscience, University of Nebraska Medical Center, Omaha, Nebraska

Received June 24, 2014; accepted August 25, 2014

ABSTRACT

Efavirenz (EFV) is a non-nucleoside reverse-transcriptase inhibitor in wide use for the treatment of human immunodeficiency virus infection. Although EFV is generally well tolerated, neuropsychiatric toxicity has been well documented. The toxic effects of EFV in hepatocytes and keratinocytes have been linked to mitochondrial perturbations and changes in autophagy. Here, we studied the effect of EFV on mitochondria and autophagy in neuronal cell lines and primary neurons. In SH-SY5Y cells, EFV induced a drop in ATP production, which coincided with increased autophagy, mitochondrial fragmentation, and mitochondrial depolarization. EFV-induced mitophagy was also detected by colocalization of mitochondria and autophagosomes and use of an outer mitochondrial membrane tandem fluorescent vector. Pharmacologic inhibition of autophagy with 3-methyladenine increased the cytotoxic effect of EFV, suggesting that autophagy promotes cell survival. EFV also reduces ATP production in primary neurons, induces autophagy, and changes mitochondrial morphology. Overall, EFV is able to acutely induce autophagy and mitochondrial changes in neurons. These changes may be involved in the mechanism leading to central nervous system toxicity observed in clinical EFV use.

Introduction

Human immunodeficiency virus (HIV) infection, in addition to causing a progressive deficiency of the immune system, can cause central nervous system (CNS) damage. The damage can range from mild cognitive impairment to severe dementia. Advances in HIV treatment have significantly reduced the burden of neurocognitive deficiency (Clifford and Ances, 2013). Combination antiretroviral therapy (cART) has drastically reduced the morbidity and mortality associated with HIV; however, the disease has become a chronic condition requiring long-term antiretroviral treatment (Deeks et al., 2013). Chronic cART therapy has highlighted long-term complications which include several CNS side effects (Carr and Cooper, 2000). Current HIV treatment combinations normally include a non-nucleoside reverse-transcriptase inhibitor (NNRTI). NNRTIs are highly potent; they can lower viral loads and increase patient $CD4^+$ T-cell counts. A NNRTI is usually administered in combination with a backbone of two nucleoside analogs (Thompson et al., 2010). Efavirenz (EFV) is the most widely used NNRTI and is recommended for use in treatment-naïve patients. EFV is generally well tolerated but does cause significant CNS side effects, including insomnia, confusion, agitation, amnesia, euphoria, and vivid dreams (Abers et al., 2014). Adverse CNS effects interfere with patient adherence and cause EFV intolerance; however, the etiology of this effect is not understood. EFV is CNS-penetrable (Letendre, 2011); therefore, EFV may contribute to primary neuronal pathology. In addition, EFV treatment has proinflammatory effects (Davidson et al., 2013). Here, we examined the effect of EFV in neuronal cell lines and primary neurons. In particular, we investigated the effect of EFV on neuronal mitochondria and autophagy.

Neuronal mitochondria are essential for growth and survival. Neurons rely on mitochondria for ATP production, intracellular Ca^{2+} homeostasis, synaptic function, and initiation of cell death (Lee, 2012). These neuronal functions are all dependent on the coordination of mitochondrial fusion and fission, mitochondrial bioenergetic function, and mitochondrial trafficking. Several lines of evidence also suggest perturbations in neuronal mitochondrial quality control play a role in human CNS disease (Chaturvedi and Flint Beal, 2013). One of the main turnover mechanisms of neuronal mitochondria is through specific autophagy (mitophagy) (Rugarli and Langer, 2012). Macroautophagy, here referred to as autophagy, is a cellular process responsible for the processing and degradation of cellular proteins and organelles for recycling (Choi et al., 2013). The autophagic process is regulated by a highly

This work was supported by the National Institutes of Health National Institute of Mental Health [Grants R01-MH073490-11 and P30-MH062261-14]. P.R.P. is supported by a University of Nebraska Medical Center fellowship.
dx.doi.org/10.1124/jpet.114.217869.

ABBREVIATIONS: cART, combination antiretroviral therapy; CCCP, carbonyl cyanide m-chlorophenyl hydrazine; CISD1, CDGSH iron-sulfur domain-containing protein 1; CNS, central nervous system; DAPI, 4′,6-diamidino-2-phenylindole; DMEM, Dulbecco's modified Eagle's medium; DMSO, dimethylsulfoxide; E18, embryonic day 18; EFV, efavirenz; EGFP, enhanced green fluorescent protein; GFP, green fluorescent protein; HIV, human immunodeficiency virus; JC-1, 5,5′,6,6′-tetrachloro-1,1′,3,3′-tetraethylbenzimidazolylcarboctanine iodide; LC3, microtubule-associated protein 1A/1B-light chain 3; LDH, lactate dehydrogenase; 3MA, 3-methyladenine; mRFP, monomeric red fluorescent protein; mTOR, mechanistic target of rapamycin; NNRTI, non-nucleoside reverse-transcriptase inhibitor; tf, tandem fluorescence.

conserved group of autophagy-related proteins. Autophagy can be identified with the phosphatidylethanolamine-conjugated form of LC3 (microtubule-associated protein 1A/1B-light chain 3) (LC3-II) (Klionsky et al., 2012). LC3-II is present in autophagosomes and can be visualized microscopically by LC3 puncta. Autophagy inhibitors, including 3-methyladenine (3MA), can suppress autophagy through direct inhibition of the phosphatidylinositol 3-kinases (Seglen and Gordon, 1982). Other groups have shown EFV induces autophagy and increases mitochondrial mass in hepatic cells (Apostolova et al., 2011). In human keratinocytes, EFV leads to cell death by the induction of autophagy through p53 (Dong et al., 2013). EFV also inhibits mitochondrial complex IV activity in mice (Streck et al., 2011). The bioenergetic effects of EFV in neurons have recently been demonstrated (Funes et al., 2014). Because of the critical role that autophagy plays in postmitotic cells, such as neurons (Nixon, 2013), we sought to determine the effect of EFV on neuronal autophagy.

By assessing ATP levels and lactate dehydrogenase (LDH) release in neuronal cell lines, we determined that EFV induces an acute drop in ATP production without an increase in cell death. This effect corresponds to the induction of autophagy, a change in mitochondrial morphology, and mitophagy. In primary neurons, EFV causes a similar drop in ATP levels with concurrent mitochondrial fragmentation, perinuclear mitochondrial clustering, and autophagy. These results suggest autophagy and mitochondrial changes are involved in the CNS effects seen with EFV treatment.

Materials and Methods

Chemicals and Cell Lines. Efavirenz was obtained through the National Institutes of Health (NIH) AIDS Reagent Program, Division of AIDS, National Institute of Allergy and Infectious Diseases (Germantown, MD). Five millimolar stock solutions of EFV were made in dimethylsulfoxide (DMSO) and stored at −80°C. Carbonyl cyanide m-chlorophenyl hydrazine (CCCP) was purchased from Tocris (Bristol, UK) and diluted in 95% ethanol. 3MA (Sigma-Aldrich, St. Louis, MO) was diluted in DMSO (5 μM stock). The neuroblastoma cell line SH-SY5Y was obtained from the American Type Culture Collection (Manassas, VA) and cultured in Dulbecco's modified Eagle's medium (DMEM)/F12 (Life Technologies, Grand Island, NY) with 10% fetal bovine serum and L-glutamine.

ATP Assay. Cellular ATP levels were measured using the CellTiter Glo Luminescent Assay (Promega, Madison, WI). Twenty-four hours before the assay, SH-SY5Y cells were seeded in 96-well tissue culture plates at 10,000 cells per well in standard DMEM/F12 media. EFV concentrations from 0 to 50 μM were prepared in DMEM/F12 media (US Biologic, Salem, MA) with glucose and without glucose, supplemented with galactose (Sigma-Aldrich). Glucose-free medium was used in all mitochondrial toxicity (ATP) assays to prevent use of glycolysis for energetic needs, and to force cells to use oxidative phosphorylation for ATP production (Rodriguez-Enriquez et al., 2001). Cells were then incubated with EFV for 2 hours (all wells contained 0.1% DMSO), followed by the addition of 2× ATP detection reagent for 10 minutes while shaking. Luminescence was measured on a FL600 plate reader (Bio-Tek Instruments, Winooski, VT). Percentage of vehicle control was calculated by dividing experimental values by vehicle-treated control wells.

JC-1 Staining. JC-1 (5,5′,6,6′-tetrachloro-1,1′,3,3′-tetraethylbenzimidazolylcarboctanine iodide) dye (Invitrogen, Grand Island, NY) was used as an indicator of mitochondrial membrane potential (Reers et al., 1995). Stock solutions of JC-1 (3 mg/ml) were made in DMSO and diluted to a final concentration of 3 μg/ml in cell culture media before a 20-minute incubation at 37°C. Cells were then rinsed twice with warmed media before adding EFV. Media only (negative controls) and 1 μM CCCP (positive controls) were used to ensure responsiveness of dye to mitochondrial depolarization (Fig. 1, D and E). Using a Zeiss 710 LSM laser scanning confocal microscope (Zeiss, Thornwood, NY) equipped with an incubation chamber, live SH-SY5Y cells were excited at 488 nm followed by detection of green JC-1 monomers with emission at 520 nm and red JC-1 aggregates with emission at 590 nm.

Imaging Autophagy and Mitochondria in SH-SY5Y Cells. SH-SY5Y cells stably expressing green fluorescent protein (GFP)-LC3 (Kabeya et al., 2000) were generated by transfection followed by GFP enrichment with flow cytometry. Cells were grown and maintained in media containing G418 (400 μg/ml). For mitochondrial imaging, cells were incubated with MitoTracker Deep Red FM (50 nM; Invitrogen) for the last 15 minutes of EFV treatments. Cells were then fixed for 20 minutes with 3.7% paraformaldehyde, and coverslips were mounted with ProlongGold DAPI (4′,6-diamidino-2-phenylindole; Invitrogen). Slides were imaged on a Zeiss 710 confocal laser scanning microscope at 63× using Zeiss Zen imaging software. An observer blinded to treatments counted individual cells containing GFP-LC3 puncta.

Generation of pCISD1–Tandem Fluorescence Vector. To make a tandem fluorescence (tf) marker for mitochondria, LC3 was removed from ptf-LC3 (Kimura et al., 2007) by double digestion with BglII and BamHI followed by ligation without LC3. The CDGSH iron-sulfur domain-containing protein 1 (*CISD1*) open reading frame from Origene (Rockville, MD) was polymerase chain reaction amplified, digested, gel purified, and inserted upstream (N terminus) to the monomeric red fluorescent protein–enhanced GFP (mRFP-EGFP; tandem fluorescent) cassette. The pCISD1-tf vector was sequenced in both directions to ensure the *CISD1* sequence was complete and in frame. CISD1, mRFP, and EGFP expression were verified by Western blotting and immunofluorescence.

LDH Assays. SH-SY5Y cells were plated at 10,000 cells per well in 96-well tissue culture plates. The next day, cells were incubated with EFV or 3MA for the times and doses stated. The Cytotoxicity Detection Kit (Roche, Madison, WI) was used, following the standard protocol. After incubation with compounds, cell medium was removed to a new 96-well plate. LDH detection reagent was added followed by incubation, in the dark, for 15 minutes at room temperature. Absorbance at 490 nM was measured on a FL600 plate reader (Bio-Tek Instruments). LDH percent cytotoxicity was calculated as follows: (experimental treatment–DMSO alone)/(1% Triton X-100–DMSO alone) × 100. Media alone, vehicle alone, and 1% Triton X-100–containing wells were included in each experiment; all treatments were done in triplicate with at least two biologic replicates.

Rat Striatal Neuron Isolation. All animal work was done following the NIH Guide for Care and Use of Laboratory Animals under University of Nebraska Medical Center Institutional Animal Care and Use Committee protocols. Striatal neurons were isolated similarly to previously established protocols (Banker and Goslin, 1998). The striatum was microdissected from embryonic day 18 (E18) Sprague-Dawley rats (Charles River, Wilmington, MA), rinsed in Hanks' balanced salt solution, and incubated with 0.5% trypsin for 30 minutes. Cells were then rinsed, triturated, resuspended in neuronal media [Neurobasal (Invitrogen) supplemented with B27 and L-glutamine], and plated on poly-D-lysine and laminin-coated tissue culture surfaces or coverslips. Medium was replaced 30 minutes after plating to remove any cellular debris. For all assays, cells were plated at a density of 25,000 cells per 12 mm in 24-well plates or 1×10^6 cells per well in six-well plates. Medium was half exchanged every 3 days and at the time of treatments. All treatments in neurons were done at day in vitro 14.

Neuronal Imaging. At day in vitro 14, neuronal medium was half exchanged with EFV to the indicated doses. For visualization of neuronal mitochondria, CellLight Mitochondria GFP (Invitrogen) was added 24 hours before treatments, or with MitoTracker Green (50 nM; Invitrogen) 15 minutes before fixation. After treatments, neurons on coverslips were rinsed and fixed in 3.7% paraformaldehyde. For visualization of LC3 in neurons, cells were fixed, rinsed, and permeabilized

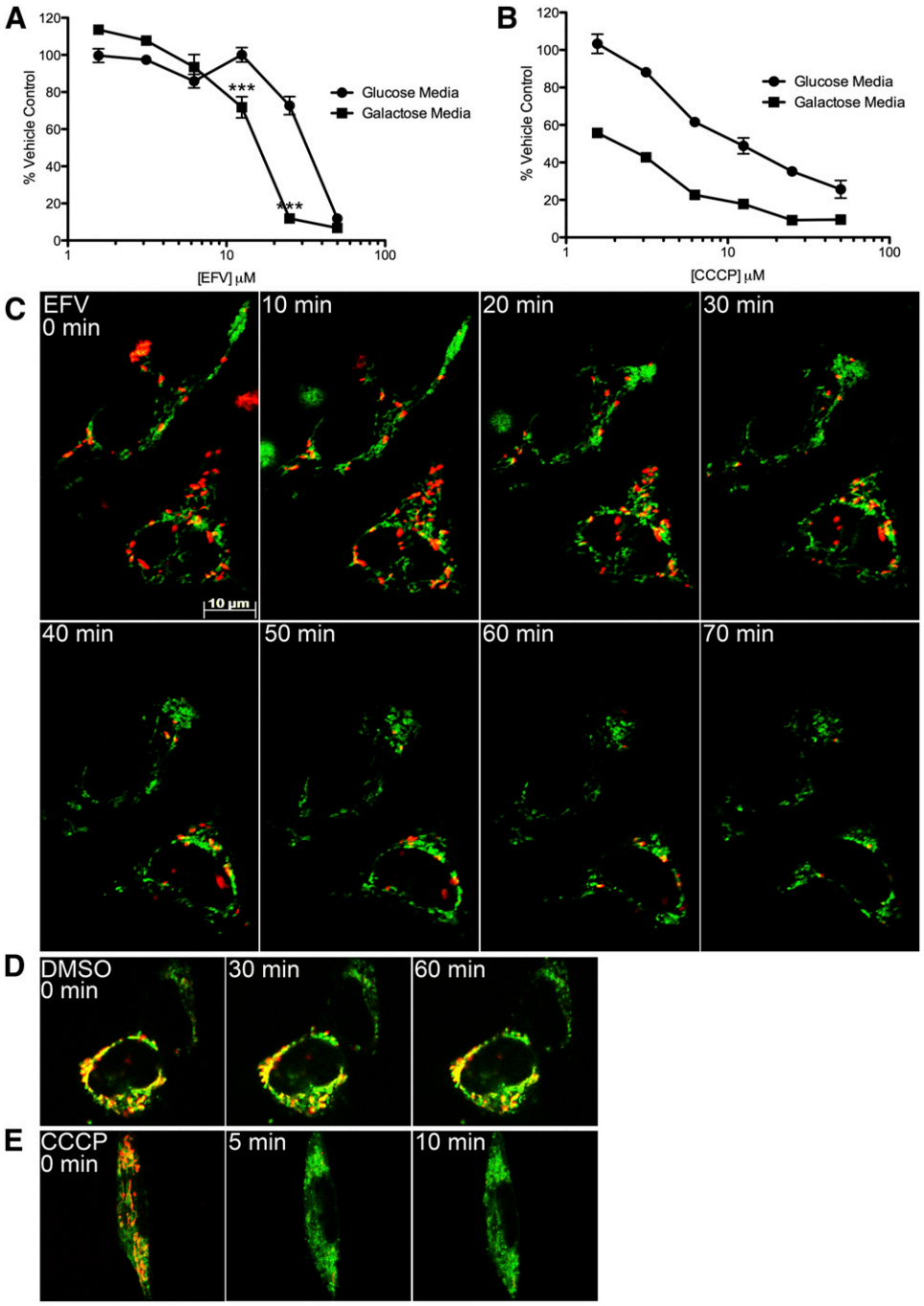

Fig. 1. Effect of EFV on ATP content in SH-SY5Y cells. (A) The cells were incubated for 2 hours with EFV in glucose-containing or glucose-free galactose-containing media at stated concentrations (50, 25, 12.5, 6.25, 3.125, and 1.5 μM). The level of ATP is given as a percentage of vehicle-treated (DMSO) cells. (B) Cells were incubated with increasing doses of CCCP for 2 hours. (C) SH-SY5Y cells were incubated with JC-1 dye followed by incubation with EFV (5 μM) for the times indicated. A high percentage of green mitochondria indicate depolarization. (D and E) SH-SY5Y cells were incubated with DMSO (no change) or CCCP (rapidly depolarized) for the times indicated. ***$P < 0.001$ galactose compared with glucose media, two-way analysis of variance followed by Bonferroni's post-tests.

with 0.1% Triton X-100. Cover slips were then blocked, rinsed, and incubated with an anti-LC3 antibody (PM036, 1:1000; MBL International, Woburn, MA) for 2 hours at room temperature followed by incubation with AlexaFluor 488 (A110088, 1:2000; Invitrogen) for 30 minutes. Coverslips were mounted with ProlongGold DAPI. All images were taken on a Zeiss LSM 710 laser scanning confocal microscope using the Zeiss Zen software.

Immunoblotting. Western blotting was performed as previously described (Purnell and Fox, 2013). Neurons were harvested in CelLytic M (Sigma-Aldrich), lysed, sonicated, and centrifuged. Supernatant was quantified and equal amounts of protein were loaded onto 4–12% bis-tris gels (Invitrogen). The primary antibodies used were as follows: p62 (1:5000; MBL International), LC3 (1:5000; MBL International), phospho-4EBP1 (Thr37/46) (1:2500; Cell Signaling Technology, Danvers, MA), and actin (1:20,000; Sigma-Aldrich). All chemiluminescent images were captured on a Carestream ImageStation 4000MM (Carestream, Rochester, NY).

Statistical Analyses. Where indicated, experiments were performed at three independent times; values represent the mean plus standard error of triplicate experiments. Two-tailed P values <0.05 were considered significant.

Results

EFV Reduces ATP Production in SH-SY5Y Cells. Because EFV has shown mitotoxic effects in other cellular systems (Blas-Garcia et al., 2010), we assessed absolute levels of ATP in SH-SY5Y neuroblastoma cells after incubation with EFV (Fig. 1A). Highly proliferative cell lines often produce

much of their ATP through glycolysis. In the presence of glucose, these cells can be resistant to known mitotoxins (Swiss and Will, 2011); therefore, we used both glucose-containing media and glucose-free media with galactose to ensure cells use oxidative phosphorylation during ATP assays. The effect of EFV on ATP levels in glucose-free media was more pronounced (Fig. 1A). This is similar to what is seen in SH-SY5Y cells treated with CCCP, a well characterized mitotoxin (Fig. 1B). This suggests that EFV has a similar mitochondrial effect. At 12.5 μM EFV, a 28% drop in ATP levels is seen after 2 hours. Increasing the EFV dose to 25 μM decreases the ATP production more than 80%. At 50 μM, the ATP level in both the glucose and galactose media is reduced more than 88%. This suggests nonmitochondrial cytotoxic mechanisms are occurring at this higher concentration (Marroquin et al., 2007).

EFV Induces Mitochondrial Depolarization. To assess if changes in mitochondrial ATP production coincide with mitochondrial depolarization, SH-SY5Y cells were incubated with JC-1 dye. JC-1 is a widely used indicator of mitochondrial polarization (Smiley et al., 1991). When mitochondria are well polarized, JC-1 aggregates in mitochondria fluorescing red. In mitochondria with low membrane potential, JC-1 remains in the monomeric form, which fluoresces green. When SH-SY5Y cells are incubated with EFV (5 μM), the number of polarized mitochondria decreases after 30 minutes (Fig. 1C). The mitochondria of vehicle-treated (0.1% DMSO) cells remain polarized (Fig. 1D). As a positive control, CCCP (1 μM) depolarizes SH-SY5Y mitochondria in 5–10 minutes (Fig. 1E).

EFV Induces Mitochondrial Morphology and Autophagy Changes in SH-SY5Y Cells. Because of the observed decreases in ATP and mitochondrial depolarization, changes in mitochondrial morphology were assessed after EFV. SH-SY5Y cells stably transfected with GFP-LC3 (to mark autophagic puncta) were used for these experiments. SH-SY5Y cells without EFV exhibited a characteristic mix of various-sized elongated mitochondria (Fig. 2A). After 2 hours of EFV treatment, mitochondria take on spheroid morphology as others have shown in depolarized mitochondria (Fig. 2B) (Ding et al., 2012). At 4 and 24 hours, there is extensive mitochondrial fragmentation and perinuclear mitochondrial clustering (Fig. 2, C and D).

In addition to mitochondrial morphology, we assessed changes in autophagy after EFV treatment. Most SH-SY5Y cells have fewer than two puncta (an indicator of autophagic vesicles) per cell before EFV treatment (Fig. 2, A, E, and F). At 2 hours, EFV increases the percentage of cells with more than two puncta. This does not reach significance and does not change the overall number of puncta per cell (Fig. 2, B, E, and F). At both 4 and 24 hours of EFV treatment, there is a significant increase in the number of puncta per cell ($P < 0.001$) (Fig. 2, C–E); the number of cells with more than two puncta was also increased at these time points (Fig. 2F). When the autophagic puncta and mitochondria are overlaid, there is an increased overlap at 4 and 24 hours, suggesting induction of mitophagy in these cells (Fig. 2, C and D, insets, white arrows).

Outer Mitochondrial Membrane Protein CISD1 Localizes to an Acidic Cellular Compartment after Incubation with EFV. To further investigate EFV-induced mitophagy, a vector (pCISD1-tf) was created by fusing the integral outer mitochondrial membrane protein CISD1 (mitoNEET) to the tandem fluorescent mRFP-EGFP tag. GFP is more sensitive to acidic environments, such as the autophagolysosome; therefore, both GFP (green) and RFP (red) will express (yellow) when this outer mitochondrial membrane protein is not in the autophagolysosome. In acidic environments, such as the autophagolysosome, only red will be seen. Before EFV, SH-SY5Y mitochondria have normal elongated shapes with coexpression of GFP and RFP (yellow) (Fig. 3A). After 2 hours of EFV (5 μM), some mitochondria remain elongated while others become punctate (Fig. 3B). Mitochondria become punctate and perinuclear after 4 hours of EFV (Fig. 3C). In addition, CISD1 is no longer fluorescing green, only red, indicating mitophagy (Fig. 3C, white arrows).

Blocking Autophagy Increases LDH Release by SH-SY5Y Cells after Incubation with EFV. To ensure that the effects of EFV are not due to cell death, release of LDH was assessed after 2 and 24 hours of EFV treatment. Further, to assess if autophagy acts as a mechanism of survival or death, 3MA was used to block autophagy. After 2 hours, EFV alone causes a 10.5% increase in LDH release at 10 μM and 11.3% at 25 μM; 3MA alone (5 μM) causes a 6.9% increase in LDH release (Fig. 3D). The combination of 10 μM EFV and 3MA causes a 20.4% LDH release; 25 μM EFV and 3MA causes a release of 19.3%. At 2 hours, 50 μM EFV has some cytotoxicity (26%), which is increased to 46% after the addition of 3MA (Fig. 3D). At 24 hours, there are still relatively low levels of LDH release at 10 μM (11.4%) and 25 μM (13.5%); however, the addition of 3MA did not increase LDH release. The effect of 3MA alone was similar (4.8%) (Fig. 3E).

ATP Levels Are Lowered in Primary Neurons after Incubation with EFV. To confirm these effects translate to primary neurons, EFV was studied in E18 rat striatal neurons. As shown in Fig. 4A, doses above 6.25 μM lower ATP levels in these neurons at 2 hours. At 12.5 μM, ATP levels are decreased by 25%; at 25 μM, ATP is lowered by 66%. At 24 hours, higher doses (50 μM) still reduce ATP; however, the effect of 12.5 and 25 μM is diminished at 24 hours (Fig. 4A). To consider the cytotoxicity caused by EFV in these primary neurons, we performed LDH assays in conjunction with the ATP assays shown. At 2 hours, LDH release was no higher than 5.2% for all doses tested (1.5–50 μM) (Fig. 4B). At 24 hours, LDH release was less than 3% for all doses less than 50 μM, which had 44% cytotoxicity (Fig. 4B).

EFV Induces Mitochondrial Fragmentation in Neurons. After observing changes in ATP similar to the SH-SY5Y cell line model, we evaluated mitochondrial morphology in EFV-treated neurons. Neurons incubated with DMSO alone (as well as untreated neurons) have elaborate, elongated mitochondrial networks (Fig. 4C). After 2 hours of 100 nM EFV, neuronal mitochondria look similar with some reduced elongation (Fig. 4D). At both 1 and 10 μM, there is extensive mitochondrial fragmentation similar to that found in SH-SY5Y cells (Fig. 4, E and F).

EFV Induces Autophagy in Rat Striatal Neurons. To confirm the induction of autophagy in these primary neurons, we treated E18 rat striatal neurons for 2 hours with doses from 0 to 10 μM EFV. We found a dose-dependent induction of autophagy, as demonstrated by increased levels of LC3-II, at all doses above 100 nM (Fig. 5A). At doses of 1 and 10 μM, there is also decreased p62 (SQSTM1, a protein turned over by

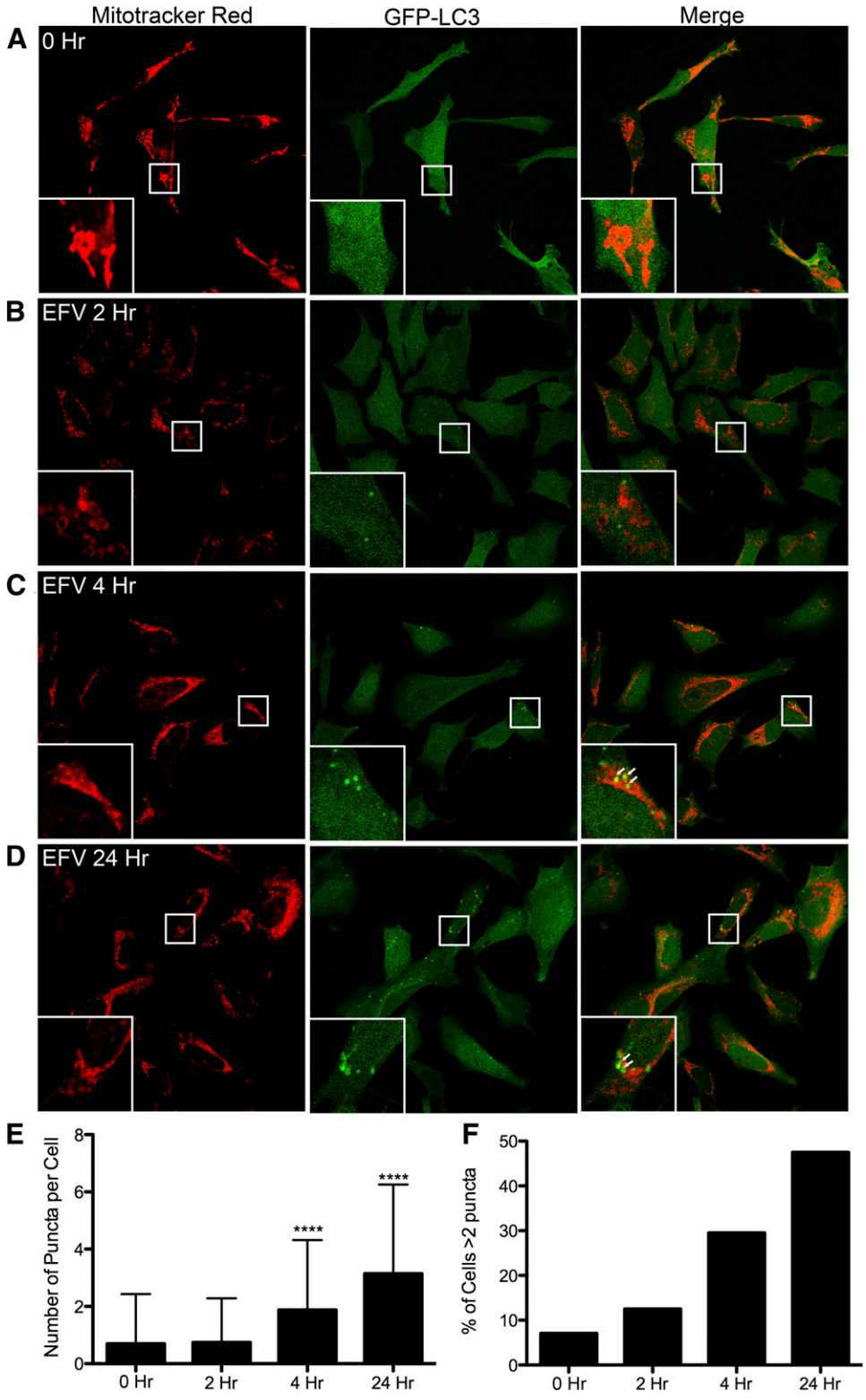

Fig. 2. EFV changes mitochondrial morphology and induces autophagy. Immunofluorescent images of mitochondria and LC3 in SH-SY5Y cells incubated with 5 μM EFV for the times indicated. Mitochondria were visualized with MitoTracker Deep Red FM (Red), and GFP-LC3 was stably transfected. (A) SH-SY5Y cells before EFV treatment. (B–D) SH-SY5Y cells incubated with EFV for the times indicated. Note the increase in autophagic puncta formation after 4 and 24 hours. Arrows (C and D insets): Areas of colocalization of mitochondria and LC3 (mitophagy). (E) Total number of GFP-LC3 puncta per cell was counted after incubation with EFV for the times indicated ($n = 200$ cells). (****$P < 0.001$ compared with untreated cells, one-way analysis of variance, followed by Bonferroni's post tests). (F) Percentage of cells with more than two puncta per cell after EFV exposure for the indicated times ($n = 200$ cells).

autophagy) suggesting increased autophagic activity (Bjorkoy et al., 2009). The mechanistic target of rapamycin (mTOR) kinase is a key controller of autophagy; mTOR inactivation by rapamycin induces autophagy in neurons in culture and in several animal models (Garelick and Kennedy, 2011). Therefore, we next examined 4EBP1, one of the main phosphorylation targets of mTOR (Carrera, 2004). After 2 hours of EFV, we see decreased phosphorylation of 4EBP1 at the mTOR phosphorylation sites (Thr37/46). In addition to detection of these autophagic markers by immunoblotting, immunofluorescence for LC3 was done to examine the formation of autophagic puncta. DMSO-treated cells have a diffuse nonpunctate LC3 localization (Fig. 5B). At 10 and 100 nM, there is increased punctate LC3 staining in the neuronal processes (Fig. 5, C and

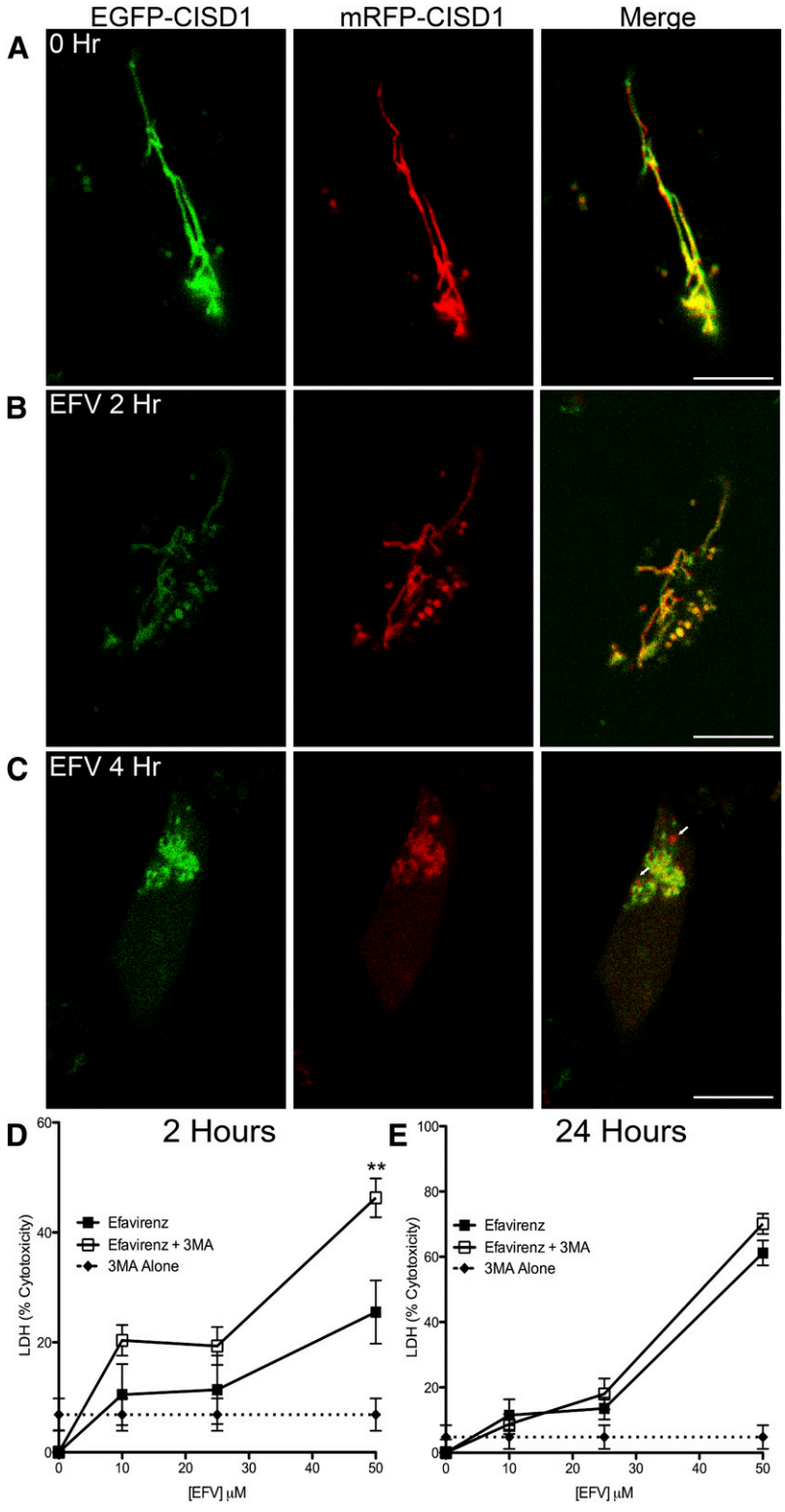

Fig. 3. Induction of mitophagy by EFV and inhibition of autophagy increases cytotoxicity. SH-SY5Y cells were transfected with p*CISD1*-tf followed by treatment with EFV for the times indicated. Immunofluorescent images of live cells were taken in both green and red channels. (A) SH-SY5Y cells before treatment. (B and C) SH-SY5Y cells after 2 and 4 hours of EFV treatment. Arrows (C): Red-only areas indicating mitochondria localized to an acidic cellular compartment, such as the autophagolysosome. (D) SH-SY5Y cells were treated with EFV (at the doses indicated), 3MA (5 μM), or EFV + 3MA for 2 hours followed by LDH assays. (E) LDH assay after 24 hours of the indicated treatments. $^{**}P < 0.01$ EFV + 3MA compared with EFV or 3MA alone, two-way analysis of variance followed by Bonferroni's post tests.

D). At 1 and 10 μM EFV, there is extensive punctate LC3 throughout all of the neuronal processes (Fig. 5, E and F).

Discussion

Understanding the etiology of acute CNS neuropsychiatric adverse effects is vital due to the wide use of EFV in cART (Decloedt and Maartens, 2013). Here, we investigated the acute effects of EFV on mitochondrial ATP production, mitochondrial morphology, and autophagy in SH-SY5Y cells and neurons. The role of abnormal mitochondria in neurodegeneration is becoming clearer (Lezi and Swerdlow, 2012). There is significant evidence implicating mitochondrial dysfunction in neurodegenerative diseases including

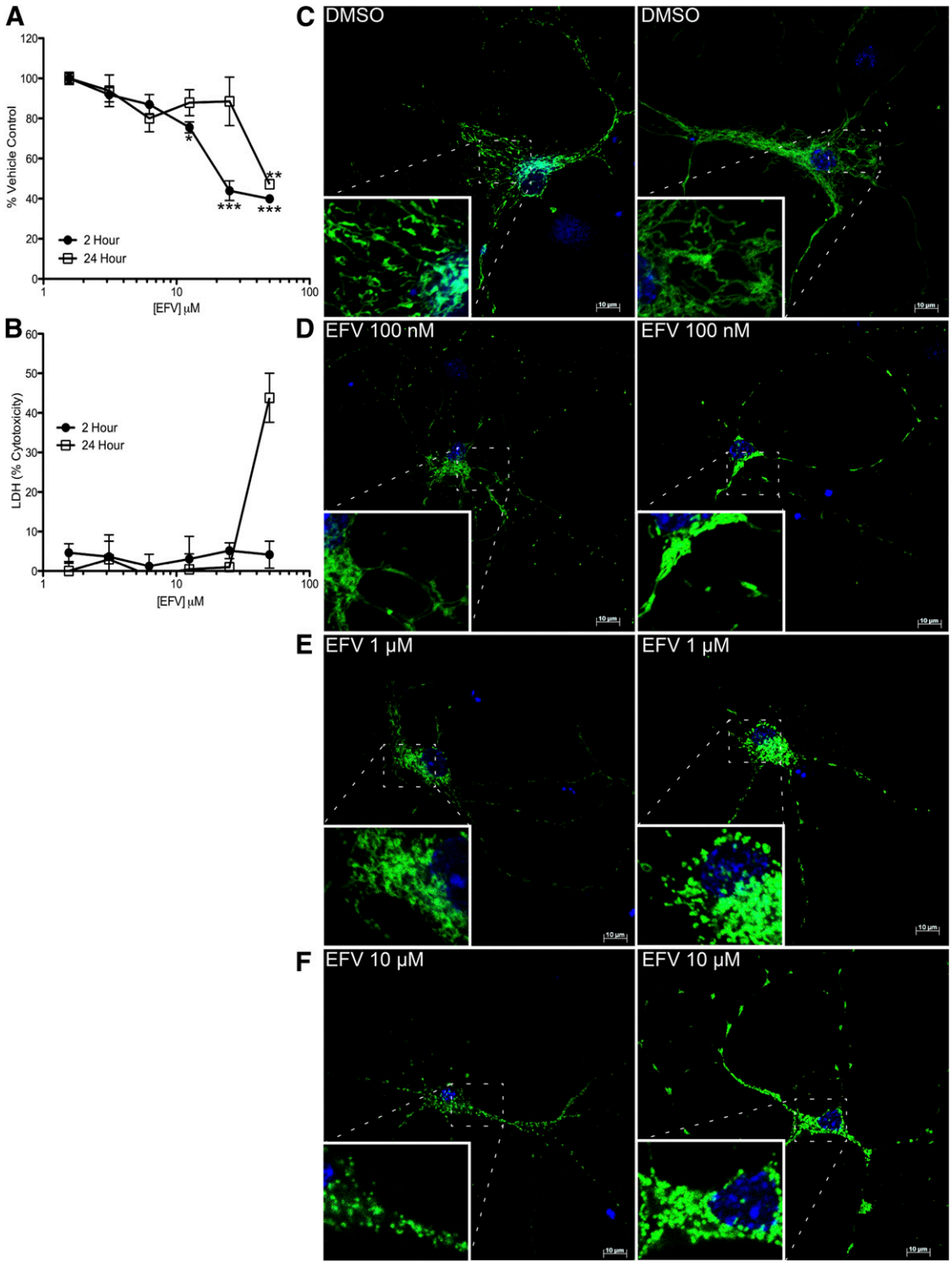

Fig. 4. ATP production and mitochondrial morphology in rat striatal neurons with EFV. (A) ATP assay in primary rat striatal neurons treated with 50, 25, 12.5, 6.25, 3.125, and 1.5 μM EFV for 2 and 24 hours. (B) LDH assay of rat striatal neurons treated with the same doses of EFV for 2 and 24 hours. (C–F) Confocal images of primary rat striatal neurons treated with the indicated doses of EFV for 2 hours with MitoTracker green for the last 15 minutes of treatment. Note the change of mitochondria to more fragmented morphology (bars = 10 μm). *$P < 0.05$; **$P < 0.01$; ***$P < 0.001$ compared with vehicle-treated neurons, one-way analysis of variance followed by Dunnett's post tests.

Parkinson's disease, Huntington's disease, Alzheimer's disease, and amyotrophic lateral sclerosis. As HIV infection becomes a chronic disease with increased levels of chronic inflammation (Deeks et al., 2013), it may mirror some of the CNS degeneration seen in these diseases. In addition, there are several lines of clinical evidence that link changes in mitochondria to neuropsychiatric abnormalities (Anglin et al., 2012). We assessed mitochondrial function after EFV exposure with ATP assays and visualization of mitochondrial morphology.

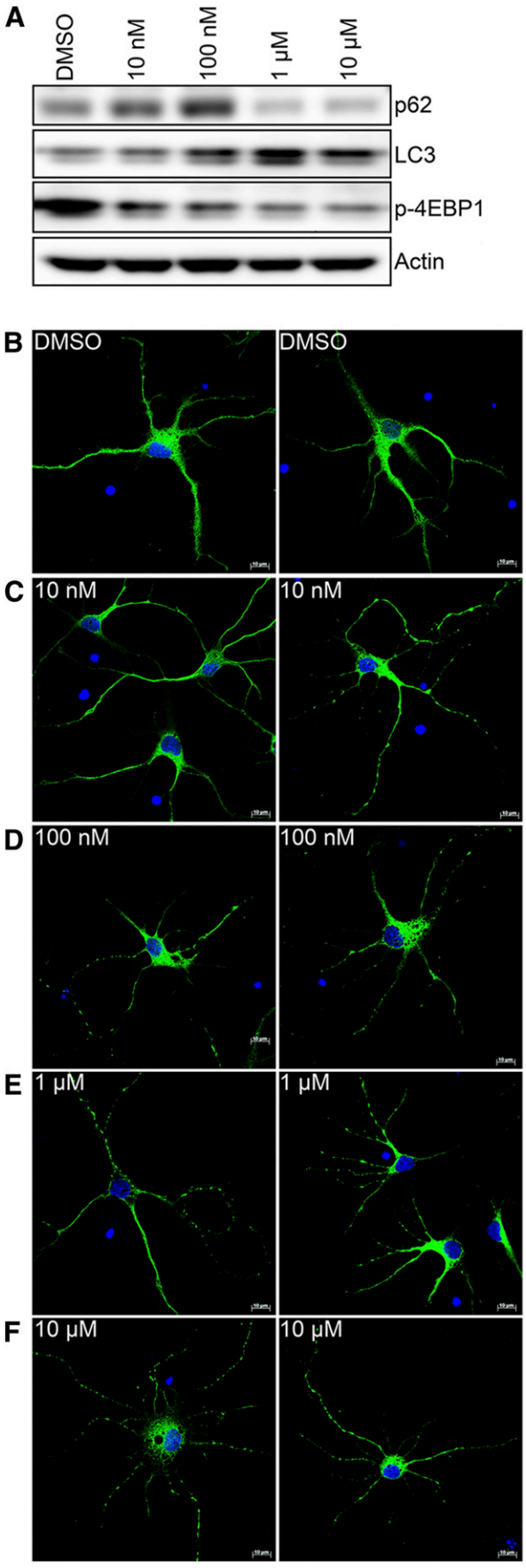

In SH-SY5Y cells, there is an acute drop in ATP levels after 2 hours of treatment with EFV (Fig. 1A). This drop in ATP production after EFV is attenuated in media containing glucose, where the cell can undergo the Crabtree effect (Marroquin et al., 2007; Diaz-Ruiz et al., 2011). This allows the cell to bypass the need for oxidative phosphorylation for energy by utilizing the glucose in culture media (Diaz-Ruiz et al., 2011). In addition, mitochondrial morphology changes to a predominantly spheroid shape after 2 hours of EFV (Fig. 2B). At 4 and 24 hours, mitochondrial morphology becomes fragmented, and mitochondria localize to perinuclear regions (Fig. 2, C and D). This is similar to what has been observed with other neuronal insults (Grohm et al., 2010; Kopeikina et al., 2011).

Concurrent with the observed changes in mitochondria, EFV induces autophagy as seen with an increased number of autophagic puncta in stably transfected GFP-LC3 SH-SY5Y cells (Fig. 2, C and D). These data are in line with the work of several groups demonstrating that mitochondrial dysfunction can lead to autophagy in neuronal models (Vives-Bauza et al., 2010; Yu et al., 2011; Cai et al., 2012; Zhang et al., 2013). There is still, however, controversy as to whether mitochondrial dysfunction alone is enough to induce autophagy. Further, the link between mitochondria and specific autophagy is probably more complicated than has been characterized (Sterky et al., 2011; Van Laar et al., 2011; Grenier et al., 2013). Here, it appears that the mitochondrial dysfunction is tied to autophagy, as mitophagy is observed after exposure to EFV. After 4 hours, we observed colocalization of mitochondria and autophagic puncta (Fig. 2, C and D). In addition, we generated a plasmid that expresses the outer mitochondrial membrane protein CISD1 (mitoNEET) with a C-terminal tandem fluorescent tag (mRFP-EGFP), in the same vein used for the visualization of LC3 (Kimura et al., 2007). Using this plasmid, we also visualized mitophagy after 4 hours of EFV (Fig. 3C). The physiologic function of autophagy is connected to cellular homeostasis, and many cell types, including neurons, use autophagy as a mechanism of survival from cellular stressors (Narendra et al., 2008; Dagda et al., 2009). In this SH-SY5Y model, autophagy appears to have prosurvival function, as inhibiting autophagy with 3MA adds to the small amount of cytotoxicity caused by the EFV treatment alone (Fig. 3D).

Although SH-SY5Y cells are commonly used to model neurons, we wanted to ensure that these results translate directly to primary neurons. In neurons, similar declines in ATP are seen after EFV treatments without substantial LDH release (Fig. 4, A and B). In addition, extensive mitochondrial fragmentation was seen after 2 hours of EFV (Fig. 4, E and F). We also found that EFV induced autophagy in a mTOR-dependent manner as demonstrated by increased levels of LC3-II, decreased p62 levels, and decreased phosphorylation of the mTOR target 4EBP1 (Fig. 5A).

As this manuscript was in preparation, another group electronically published results in agreement with the work shown here (Funes et al., 2014). They demonstrated altered

Fig. 5. EFV induces autophagy in rat striatal neurons. (A) Rat striatal neurons were incubated with the indicated doses of EFV for 2 hours followed by immunoblotting with the indicated antibodies. (B–F) Striatal neurons were infected with mitochondrial CellLight GFP for 24 hours followed by incubation with the indicated doses of EFV for 2 hours. Shown is the immunocytochemistry for LC3.

mitochondrial respiration after EFV treatments, in addition to reactive oxygen species generation and reduced ATP levels. Further, they showed a specific phosphorylation of AMP-activated protein kinase in glia. These data, together with the work shown here, strongly suggest a primary mitotoxic effect caused by EFV in the CNS, followed by a mitophagic cellular response.

The study of EFV in neurons is important due to the chronic nature of antiretroviral therapy in HIV-positive patients, the prevalence of EFV in cART regimens, and the clinical CNS effects of EFV treatment. Our results support the idea that EFV alters mitochondrial function in neurons and can induce autophagy as shown in other cell types. In SH-SY5Y cells, the induction of autophagy appears to have a protective role. The observed effects of EFV may help to explain some of the mechanisms underlying the acute CNS neuropsychiatric side effects seen in EFV-treated patients. This work suggests mitochondrial changes and autophagy may, at least in part, be responsible for the adverse neuropsychiatric effects observed in patients.

Acknowledgments

The authors thank Dr. Kelly Stauch for scientific input and Janice Taylor and James Talaska from the University of Nebraska Medical CenterLaser Scanning Microscopy Core Facility for valuable technical assistance with microscopy. In addition, the authors thank the NIH AIDS Reagent Program, Division of AIDS, National Institute of Allergy and Infectious Diseases for providing efavirenz.

Authorship Contributions

Participated in research design: Purnell, Fox.
Conducted experiments: Purnell.
Performed data analysis: Purnell, Fox.
Wrote or contributed to the writing of the manuscript: Purnell, Fox.

References

Abers MS, Shandera WX, and Kass JS (2014) Neurological and psychiatric adverse effects of antiretroviral drugs. *CNS Drugs* **28**:131–145.
Anglin RE, Garside SL, Tarnopolsky MA, Mazurek MF, and Rosebush PI (2012) The psychiatric manifestations of mitochondrial disorders: a case and review of the literature. *J Clin Psychiatry* **73**:506–512.
Apostolova N, Gomez-Sucerquia LJ, Gortat A, Blas-Garcia A, and Esplugues JV (2011) Compromising mitochondrial function with the antiretroviral drug efavirenz induces cell survival-promoting autophagy. *Hepatology* **54**:1009–1019.
Banker G and Goslin K (1998) *Culturing nerve cells*, MIT Press, Cambridge, Mass.
Bjørkøy G, Lamark T, Pankiv S, Øvervatn A, Brech A, and Johansen T (2009) Monitoring autophagic degradation of p62/SQSTM1. *Methods Enzymol* **452**: 181–197.
Blas-García A, Apostolova N, Ballesteros D, Monleón D, Morales JM, Rocha M, Victor VM, and Esplugues JV (2010) Inhibition of mitochondrial function by efavirenz increases lipid content in hepatic cells. *Hepatology* **52**:115–125.
Cai Q, Zakaria HM, Simone A, and Sheng ZH (2012) Spatial parkin translocation and degradation of damaged mitochondria via mitophagy in live cortical neurons. *Curr Biol* **22**:545–552.
Carr A and Cooper DA (2000) Adverse effects of antiretroviral therapy. *Lancet* **356**: 1423–1430.
Carrera AC (2004) TOR signaling in mammals. *J Cell Sci* **117**:4615–4616.
Chaturvedi RK and Flint Beal M (2013) Mitochondrial diseases of the brain. *Free Radic Biol Med* **63**:1–29.
Choi AM, Ryter SW, and Levine B (2013) Autophagy in human health and disease. *N Engl J Med* **368**:651–662.
Clifford DB and Ances BM (2013) HIV-associated neurocognitive disorder. *Lancet Infect Dis* **13**:976–986.
Dagda RK, Cherra SJ, 3rd, Kulich SM, Tandon A, Park D, and Chu CT (2009) Loss of PINK1 function promotes mitophagy through effects on oxidative stress and mitochondrial fission. *J Biol Chem* **284**:13843–13855.
Davidson DC, Schifitto G, and Maggirwar SB (2013) Valproic acid inhibits the release of soluble CD40L induced by non-nucleoside reverse transcriptase inhibitors in human immunodeficiency virus infected individuals. *PLoS ONE* **8**:e59950.
Decloedt EH and Maartens G (2013) Neuronal toxicity of efavirenz: a systematic review. *Expert Opin Drug Saf* **12**:841–846.
Deeks SG, Lewin SR, and Havlir DV (2013) The end of AIDS: HIV infection as a chronic disease. *Lancet* **382**:1525–1533.
Diaz-Ruiz R, Rigoulet M, and Devin A (2011) The Warburg and Crabtree effects: On the origin of cancer cell energy metabolism and of yeast glucose repression. *Biochim Biophys Acta* **1807**:568–576.
Ding WX, Li M, Biazik JM, Morgan DG, Guo F, Ni HM, Goheen M, Eskelinen EL, and Yin XM (2012) Electron microscopic analysis of a spherical mitochondrial structure. *J Biol Chem* **287**:42373–42378.
Dong Q, Oh JE, Yi JK, Kim RH, Shin KH, Mitsuyasu R, Park NH, and Kang MK (2013) Efavirenz induces autophagy and aberrant differentiation in normal human keratinocytes. *Int J Mol Med* **31**:1305–1312.
Funes HA, Apostolova N, Alegre F, Blas-Garcia A, Alvarez A, Marti-Cabrera M, and Esplugues JV (2014) Neuronal bioenergetics and acute mitochondrial dysfunction: a clue to understanding the central nervous system side effects of efavirenz. *J Infect Dis* DOI: 10.1093/infdis/jiu273 [published ahead of print].
Garelick MG and Kennedy BK (2011) TOR on the brain. *Exp Gerontol* **46**:155–163.
Grenier K, McLelland GL, and Fon EA (2013) Parkin- and PINK1-dependent mitophagy in neurons: will the real pathway please stand up? *Front Neurol* **4**:100.
Grohm J, Plesnila N, and Culmsee C (2010) Bid mediates fission, membrane permeabilization and peri-nuclear accumulation of mitochondria as a prerequisite for oxidative neuronal cell death. *Brain Behav Immun* **24**:831–838.
Kabeya Y, Mizushima N, Ueno T, Yamamoto A, Kirisako T, Noda T, Kominami E, Ohsumi Y, and Yoshimori T (2000) LC3, a mammalian homologue of yeast Apg8p, is localized in autophagosome membranes after processing. *EMBO J* **19**:5720–5728.
Kimura S, Noda T, and Yoshimori T (2007) Dissection of the autophagosome maturation process by a novel reporter protein, tandem fluorescent-tagged LC3. *Autophagy* **3**:452–460.
Klionsky DJ, Abdalla FC, Abeliovich H, Abraham RT, Acevedo-Arozena A, Adeli K, Agholme L, Agnello M, Agostinis P, and Aguirre-Ghiso JA, et al. (2012) Guidelines for the use and interpretation of assays for monitoring autophagy. *Autophagy* **8**:445–544.
Kopeikina KJ, Carlson GA, Pitstick R, Ludvigson AE, Peters A, Luebke JI, Koffie RM, Frosch MP, Hyman BT, and Spires-Jones TL (2011) Tau accumulation causes mitochondrial distribution deficits in neurons in a mouse model of tauopathy and in human Alzheimer's disease brain. *Am J Pathol* **179**:2071–2082.
Lee JA (2012) Neuronal autophagy: a housekeeper or a fighter in neuronal cell survival? *Exp Neurobiol* **21**:1–8.
Letendre S (2011) Central nervous system complications in HIV disease: HIV-associated neurocognitive disorder. *Top Antivir Med* **19**:137–142.
Lezi E and Swerdlow RH (2012) Mitochondria in neurodegeneration. *Adv Exp Med Biol* **942**:269–286.
Marroquin LD, Hynes J, Dykens JA, Jamieson JD, and Will Y (2007) Circumventing the Crabtree effect: replacing media glucose with galactose increases susceptibility of HepG2 cells to mitochondrial toxicants. *Toxicol Sci* **97**:539–547.
Narendra D, Tanaka A, Suen DF, and Youle RJ (2008) Parkin is recruited selectively to impaired mitochondria and promotes their autophagy. *J Cell Biol* **183**:795–803.
Nixon RA (2013) The role of autophagy in neurodegenerative disease. *Nat Med* **19**: 983–997.
Purnell PR and Fox HS (2013) Autophagy-mediated turnover of dynamin-related protein 1. *BMC Neurosci* **14**:86.
Reers M, Smiley ST, Mottola-Hartshorn C, Chen A, Lin M, and Chen LB (1995) Mitochondrial membrane potential monitored by JC-1 dye. *Methods Enzymol* **260**: 406–417.
Rodríguez-Enríquez S, Juárez O, Rodríguez-Zavala JS, and Moreno-Sánchez R (2001) Multisite control of the Crabtree effect in ascites hepatoma cells. *Eur J Biochem* **268**:2512–2519.
Rugarli EI and Langer T (2012) Mitochondrial quality control: a matter of life and death for neurons. *EMBO J* **31**:1336–1349.
Seglen PO and Gordon PB (1982) 3-Methyladenine: specific inhibitor of autophagic/lysosomal protein degradation in isolated rat hepatocytes. *Proc Natl Acad Sci USA* **79**:1889–1892.
Smiley ST, Reers M, Mottola-Hartshorn C, Lin M, Chen A, Smith TW, Steele GD, Jr, and Chen LB (1991) Intracellular heterogeneity in mitochondrial membrane potentials revealed by a J-aggregate-forming lipophilic cation JC-1. *Proc Natl Acad Sci USA* **88**:3671–3675.
Sterky FH, Lee S, Wibom R, Olson L, and Larsson NG (2011) Impaired mitochondrial transport and Parkin-independent degeneration of respiratory chain-deficient dopamine neurons in vivo. *Proc Natl Acad Sci USA* **108**:12937–12942.
Streck EL, Ferreira GK, Scaini G, Rezin GT, Gonçalves CL, Jeremias IC, Zugno AI, Ferreira GC, Moreira J, and Fochesato CM, et al. (2011) Non-nucleoside reverse transcriptase inhibitors efavirenz and nevirapine inhibit cytochrome C oxidase in mouse brain regions. *Neurochem Res* **36**:962–966.
Swiss R and Will Y (2011) Assessment of mitochondrial toxicity in HepG2 cells cultured in high-glucose- or galactose-containing media, in *Current Protocols in Toxicology,* Chapter 2: Unit 2.20, Wiley, Hoboken, NJ
Thompson MA, Aberg JA, Cahn P, Montaner JS, Rizzardini G, Telenti A, Gatell JM, Günthard HF, Hammer SM, and Hirsch MS, et al.; International AIDS Society-USA (2010) Antiretroviral treatment of adult HIV infection: 2010 recommendations of the International AIDS Society-USA panel. *JAMA* **304**:321–333.
Van Laar VS, Arnold B, Cassady SJ, Chu CT, Burton EA, and Berman SB (2011) Bioenergetics of neurons inhibit the translocation response of Parkin following rapid mitochondrial depolarization. *Hum Mol Genet* **20**:927–940.
Vives-Bauza C, Zhou C, Huang Y, Cui M, de Vries RL, Kim J, May J, Tocilescu MA, Liu W, and Ko HS, et al. (2010) PINK1-dependent recruitment of Parkin to mitochondria in mitophagy. *Proc Natl Acad Sci USA* **107**:378–383.
Yu W, Sun Y, Guo S, and Lu B (2011) The PINK1/Parkin pathway regulates mitochondrial dynamics and function in mammalian hippocampal and dopaminergic neurons. *Hum Mol Genet* **20**:3227–3240.
Zhang X, Yan H, Yuan Y, Gao J, Shen Z, Cheng Y, Shen Y, Wang RR, Wang X, and Hu WW, et al. (2013) Cerebral ischemia-reperfusion-induced autophagy protects against neuronal injury by mitochondrial clearance. *Autophagy* **9**:1321–1333.

Address correspondence to: Howard S. Fox, Department of Pharmacology and Experimental Neuroscience, University of Nebraska Medical Center, 985900 Nebraska Medical Center, Omaha, NE 68198-5800. E-mail: hfox@unmc.edu